ELSEVIER

Earth and Planetary Science Letters 201 (2002) 171–186

EPSL

www.elsevier.com/locate/epsl

# Quasi-conservative behaviour of $^{10}$Be in deep waters of the Weddell Sea and the Atlantic sector of the Antarctic Circumpolar Current

M. Frank [a,b,*], M.M. Rutgers van der Loeff [c], Peter W. Kubik [d], Augusto Mangini [b]

[a] *Institute for Isotope Geology and Mineral Resources, Department of Earth Sciences, ETH Zentrum, NO F51.3, Sonneggstrasse 5, CH-8092 Zurich, Switzerland*

[b] *Heidelberg Academy of Sciences, c/o Institute for Environmental Physics, University of Heidelberg, INF 229, 69120 Heidelberg, Germany*

[c] *Alfred Wegener Institute for Polar and Marine Research, P.O. Box 120161, 27515 Bremerhaven, Germany*

[d] *Paul Scherrer Institute, c/o Institute for Particle Physics, ETH Zurich, ETH-Hönggerberg, CH-8093 Zurich, Switzerland*

Received 3 October 2001; received in revised form 16 April 2002; accepted 22 April 2002

**Abstract**

We present the first transect of dissolved $^{10}$Be depth profiles across the Antarctic Circumpolar Current (ACC) in the Atlantic sector. North of the Polar Front the $^{10}$Be concentrations increase continuously from very low values at the surface to values of up to 1600 atoms/g at depth. Deep water $^{10}$Be concentrations of particular water masses are consistent with earlier results obtained further north. South of the Polar Front and in the Weddell Sea the distribution of $^{10}$Be is also characterised by low surface concentrations but below 1000 m depth the concentrations are relatively constant and significantly higher (up to 2000 atoms/g) than further north, probably as a result of mixing and advection of water masses of Pacific origin. Overall the deep water $^{10}$Be distribution is obviously not significantly affected by scavenging processes or ice melt and comparison with the density distribution suggests that $^{10}$Be can be viewed as a quasi-conservative tracer. This provides a tool for an improved understanding of the behaviour of other more particle reactive trace metals in the Southern Ocean such as $^{230}$Th: in deep waters north of the ACC/Weddell Gyre boundary (AWB) $^{10}$Be/$^{230}$Th has a relatively constant value ($1.7 \pm 0.3 \times 10^9$ atoms/dpm) over a wide density range whereas south of the AWB the ratio is significantly lower ($1.1 \pm 0.2 \times 10^9$ atoms/dpm). This normalisation to $^{10}$Be corroborates that $^{230}$Th is enriched by 50% due to accumulation south of the AWB as a consequence of minimal particulate fluxes. The quasi-conservative behaviour deduced from our results also implies that $^{10}$Be can only be used as a tracer for Southern Ocean particle fluxes in the past if ocean circulation patterns and water mass residence times did not change significantly. 

*Keywords:* Be-10; radioactive isotopes; deep-water environment; particles; reactivity; Antarctic Ocean

* Corresponding author, at address a. Tel.: +41-1-632-3745; Fax: +41-1-632-1179.
*E-mail address:* frank@erdw.ethz.ch (M. Frank).

0012-821X/02/$ – see front matter 
PII: S0012-821X(02)00688-X

## 1. Introduction

The behaviour of the particle reactive radionuclides $^{10}$Be, $^{231}$Pa and $^{230}$Th in the oceans has been subject of numerous studies. The value of these three isotopes arises from their constant production rates, but different residence times, which allows detailed investigation of particulate fluxes and water mass advection in the present and past ocean.

Cosmogenic $^{10}$Be (half-life = 1.5 Myr) is produced at an essentially constant rate in the upper atmosphere and is then transferred to the surface ocean by precipitation. For this study we will use a global average $^{10}$Be production rate of $1.21 \pm 0.26 \times 10^6$ atoms/cm$^2$ yr [1]. Although there are latitudinal variations in the atmospheric deposition of $^{10}$Be [2], these are expected to be homogenised due to the relatively long average residence time of $^{10}$Be in the ocean of about 500–1000 yr [3–5]. The residence time is a function of the particle reactivity of $^{10}$Be and allows the buildup of nutrient-type water column profiles [6]. It also leads to a pronounced effect of boundary scavenging, i.e. $^{10}$Be is transported from low particle flux areas such as central ocean gyres to the ocean's boundaries or other high particle flux areas and is scavenged there in excess of its production rate [7,8]. In deep waters the ratio between $^{10}$Be and stable $^{9}$Be has been used to trace deep ocean circulation [9]. The $^{10}$Be/$^{9}$Be in deep waters increases with the age of the water masses, which is mainly a consequence of a 2.5-fold increase of the $^{10}$Be concentration along the deep thermohaline circulation from the deep north Atlantic to the deep north Pacific [4,6,10].

$^{230}$Th (half-life = 75 200 yr) and $^{231}$Pa (half life = 32 000 yr) are produced at constant rates of 0.0263 dpm/m$^3$ yr and 0.00 233 dpm/m$^3$ yr, respectively, by radioactive decay of U which is homogeneously distributed in the ocean. Their particle reactivities are much higher than that of $^{10}$Be leading to water column residence times on the order of 5–40 yr for Th and 50–200 yr for Pa [11–13].

These differences in residence times are accompanied by differential adsorption as a function of particulate matter composition in the ocean. Th is the most particle reactive of the three elements and shows little differential scavenging, although there have been suggestions that detrital clays may be the most efficient scavengers [14]. Pa shows an enhanced adsorption to biogenic opal [15,16]. For $^{10}$Be, efficient scavenging by detrital aluminosilicates [17,18] and biogenic opal have been discussed [19].

In the Atlantic sector of the Southern Ocean the behaviour of Th and Pa is controlled by the balance between scavenging, ingrowth and advection [20]. It has been demonstrated that $^{230}$Th is enriched in the Weddell Sea water column, which is most likely explained by the coincidence that the ventilation time ($\sim$35 yr) of the Weddell Sea by LCDW (Lower Circumpolar Deep Water, including a contribution of North Atlantic Deep Water, NADW) is of the same order as the scavenging residence time of Th, which is on average about 30 yr. This situation, stimulated by an even longer scavenging residence time within the Weddell Sea as a result of extremely low particulate fluxes, allows a buildup and finally an export of Th from the Weddell Sea to the Antarctic Circumpolar Current (ACC). A similar enrichment of $^{231}$Pa was not observed, in line with its longer average scavenging residence time of approximately 100–200 yr and the short Weddell Sea ventilation time. This does not allow the isotope to accumulate significantly during residence in the Weddell Sea. Walter et al. [21] have shown that the Th scavenging rate in the Weddell Sea is indeed reduced by approximately 60%, thus verifying the assumptions made for the modelling that gave the best fit to the $^{230}$Th data from the central Weddell Sea (station 227 in [20]).

The evaluation of the scavenging behaviour of Pa is complicated by the fact that $^{231}$Pa is advected southward from the Atlantic into the Southern Ocean [22]. South of the Polar Front the preference of Th over Pa scavenging collapses, probably as a result of enhanced Pa scavenging by biogenic opal. As a result, Pa is scavenged effectively in the Weddell Sea despite low overall particulate fluxes.

The distribution and scavenging behaviour of cosmogenic $^{10}$Be in the world ocean has many similarities to those of $^{230}$Th and $^{231}$Pa. Although

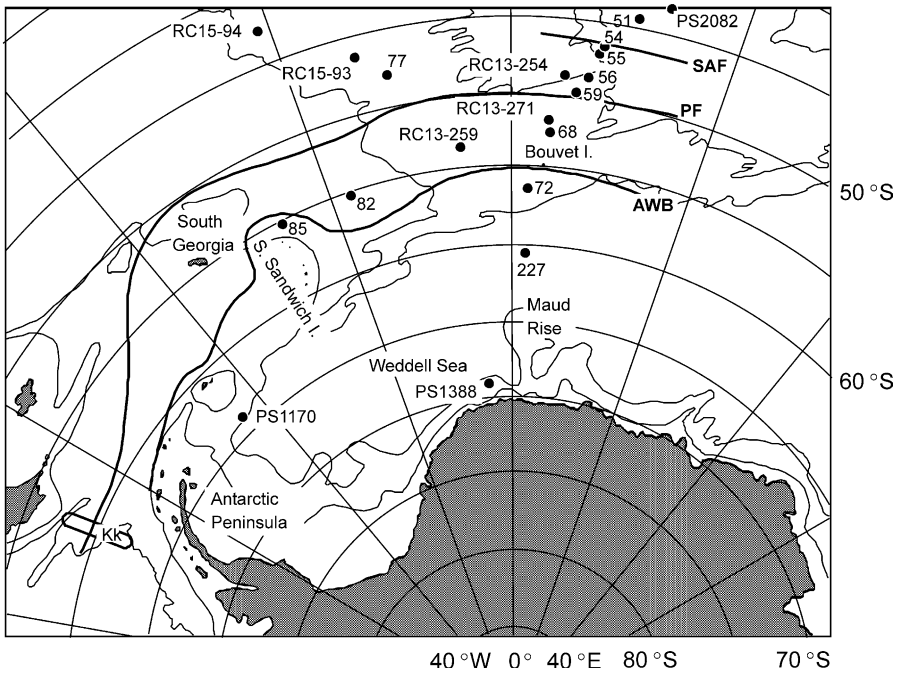


Fig. 1. Map with locations of the stations. The stations PS1751 to PS1785 are indicated by their two last digits. The positions of the Subantarctic Front (SAF) and the Polar Front (PF) east of 20°W are based on hydrographic observations during the expedition ANT VIII/3. The mean positions of the PF west of 20°W and of the ACC–Weddell Gyre Boundary (AWB) are given according to [46]. For comparison also the locations of previous water column studies of $^{10}$Be in the Southern Ocean (Kk [29]) and sediment core studies (RC cores [24]; PS1772-8, PS1768-8, PS1756-5, PS1754-1, PS2082-1 [18]; PS1170, PS1388 [39]) are indicated.

its source function is entirely different from that of the two uranium daughters all three are subject to reversible exchange with suspended particles, their scavenging flux depends on the particle rain rate, and the extent of boundary scavenging depends on the distance that can be covered during the scavenging residence time, being largest for Be and smallest for Th. Comparative studies of these elements allow insights into processes linked to particulate fluxes, scavenging preferences and advective transport within water masses in the ocean of the present day [23] and the past [24,22,18,25]. In this study we present a set of eight new water column profiles of $^{10}$Be concentrations in the Weddell Sea and the Atlantic sector of the ACC from where up to now no $^{10}$Be measurements have been available. Together with $^{230}$Th and $^{231}$Pa measurements which were obtained on the same sample set and published previously [20] and sedimentary data from similar locations [24,18] these data offer a unique opportunity to improve the understanding of the scavenging behaviour of all three radioisotopes. They allow the investigation of the relative importance of amount and material of the particulate fluxes and advective transport in the complex hydrography of the Atlantic sector of the Southern Ocean. These results also have implications for the use of $^{10}$Be, $^{230}$Th and $^{231}$Pa to reconstruct Late Quaternary particle fluxes and export productivity.

## 2. Materials and methods

During *Polarstern* expedition ANT VIII/3 in November 1989, the water column was sampled at eight stations situated along two transects across the frontal system of the ACC (Fig. 1). Details on station location and hydrography are

Table 1
Dissolved $^{10}Be$ concentrations, $^{10}Be/^{230}Th$ and $^{10}Be/^{231}Pa$ ($\pm 1\sigma$ uncertainties)

| Water depth (m) | Density ($\sigma_2$) (kg/m$^3$) | $^{10}Be$ (at/g) | $^{10}Be/^{230}Th$ ($10^9$ at/dpm) | $^{10}Be/^{231}Pa$ ($10^9$ at/dpm) |
|---|---|---|---|---|
| *PS1755* | | | | |
| 10 | 36.118 | 369 ± 90 | 2.07 ± 0.73 | – ± – |
| 100 | – | 517 ± 99 | – ± – | – ± – |
| 2500 | 37.059 | 1015 ± 322 | 1.64 ± 0.52 | 3.43 ± 1.13 |
| *PS1759* | | | | |
| 10 | 36.341 | 0 ± 0 | 0 ± 0 | – ± – |
| 100 | – | 0 ± 0 | – ± – | – ± – |
| 300 | 36.559 | 266 ± 149 | 0.82 ± 0.46 | 2.78 ± 1.67 |
| 800 | 36.838 | 898 ± 141 | 2.18 ± 0.35 | 3.55 ± 0.70 |
| 2200 | 37.077 | 1333 ± 253 | 1.70 ± 0.33 | 5.89 ± 1.32 |
| 3600 | 37.137 | 1692 ± 235 | 2.54 ± 0.36 | 4.81 ± 0.79 |
| *PS1759* | | | | |
| 10 | 36.674 | 532 ± 94 | 0.87 ± 0.17 | – ± – |
| 100 | – | 386 ± 98 | – ± – | – ± – |
| 300 | 36.806 | 792 ± 127 | 2.11 ± 0.36 | 5.38 ± 1.17 |
| 600 | 36.944 | 767 ± 146 | 1.27 ± 0.25 | 2.66 ± 0.56 |
| 1900 | 37.119 | 1188 ± 109 | 1.39 ± 0.13 | 4.41 ± 0.62 |
| 3200 | 37.170 | 1493 ± 209 | 1.46 ± 0.21 | 3.59 ± 0.61 |
| *PS1772* | | | | |
| 10 | 36.969 | 608 ± 112 | 1.05 ± 0.21 | – ± – |
| 130 | – | 512 ± 88 | – ± – | – ± – |
| 265 | – | 558 ± 141 | – ± – | – ± – |
| 400 | 37.069 | 969 ± 187 | 0.95 ± 0.18 | 3.66 ± 0.73 |
| 1600 | 37.167 | 1869 ± 277 | 1.38 ± 0.21 | 5.54 ± 0.88 |
| 2800 | 37.198 | 1621 ± 120 | 1.01 ± 0.08 | 5.26 ± 0.46 |
| 4000 | 37.207 | 1568 ± 125 | 1.03 ± 0.08 | 3.79 ± 0.35 |
| *PS1777* | | | | |
| 10 | 36.123 | 0 ± 0 | 0 ± 0 | – ± – |
| 100 | – | 367 ± 156 | – ± – | – ± – |
| 400 | 36.594 | 486 ± 131 | 1.68 ± 0.46 | 3.04 ± 0.88 |
| 900 | 36.852 | 860 ± 155 | 1.97 ± 0.36 | 3.21 ± 0.64 |
| 1650 | 37.005 | 1007 ± 166 | 1.54 ± 0.26 | 3.27 ± 0.72 |
| 2400 | 37.101 | 1144 ± 152 | 1.62 ± 0.22 | 4.54 ± 0.92 |
| *PS1782* | | | | |
| 10 | 36.522 | 290 ± 42 | 0.72 ± 0.13 | – ± – |
| 100 | – | 248 ± 29 | – ± – | – ± – |
| 600 | 37.056 | 1198 ± 117 | 1.79 ± 0.18 | 4.99 ± 0.64 |
| 2000 | 37.156 | 1936 ± 120 | 1.79 ± 0.12 | 5.45 ± 0.42 |
| 3500 | 37.197 | 2027 ± 233 | 1.82 ± 0.21 | 6.77 ± 0.82 |
| 5000 | 37.209 | 1684 ± 194 | 1.37 ± 0.16 | 4.61 ± 0.58 |
| *PS1785* | | | | |
| 10 | 36.559 | 511 ± 97 | 1.13 ± 0.23 | – ± – |
| 100 | – | 335 ± 48 | – ± – | – ± – |
| 600 | 37.072 | 1291 ± 115 | 1.83 ± 0.17 | 4.72 ± 0.67 |
| 2500 | 37.180 | 1605 ± 143 | 1.28 ± 0.12 | 5.19 ± 0.68 |
| 4000 | 37.212 | 1776 ± 142 | 1.23 ± 0.10 | 6.26 ± 0.68 |
| 5500 | 37.220 | 1329 ± 82 | 1.09 ± 0.07 | 4.19 ± 0.35 |
| 6500 | – | 2006 ± 112 | – ± – | – ± – |
| *227* | | | | |
| 25 | – | 254 ± 23 | – ± – | – ± – |
| 160 | 37.102 | 1103 ± 70 | 1.34 ± 0.10 | – ± – |
| 1300 | 37.165 | 1721 ± 112 | 1.10 ± 0.07 | 4.56 ± 0.58 |
| 2600 | 37.197 | 1724 ± 107 | 0.95 ± 0.06 | 4.06 ± 0.59 |
| 3900 | 37.219 | 1597 ± 86 | 0.90 ± 0.05 | 4.09 ± 0.42 |
| 5200 | 37.228 | 1493 ± 84 | 1.04 ± 0.06 | 4.19 ± 0.76 |

For reference we have also included the density ($\sigma_2$) from [20], where the original $^{230}Th$ and $^{231}Pa$ data and additional information for these water samples are available.

given in the cruise report [26]. Station 227 in the Weddell Sea was sampled during expedition ANT IX/3 in March 1991. This station was selected to be in the centre of the Weddell Gyre. Profiles of dissolved and particulate Th and Pa were obtained with COSS stand-alone pumps following procedures given earlier [20]. Discrete large-volume water samples were taken with Gerard bottles deployed at the same depth and on the same wire.

The samples were filtered through 142 mm 1 μm nuclepore filters and separate 20 l samples were collected for $^{10}$Be analysis. These samples were weighed, acidified with 20 ml of concentrated $HNO_3$, different yield tracers (such as $^{229}$Th and $^{233}$Pa) and 0.5 ml of a $^{9}$Be carrier (with a concentration of 1.04 mg $^{9}$Be ml$^{-1}$) were added, and 250 mg Fe carrier ($FeCl_3$) in dilute HCl were added and mixed. After a 24 h equilibration time, Th, Pa, and Be were coprecipitated as $Fe(OH)_3$ and $Mg(OH)_2$ with $NH_3$ at pH 9.5–10. The precipitate was dissolved in concentrated HCl and Th was coprecipitated as $Fe(OH)_3$ for $^{234}$Th analysis with concentrated $NH_3$ until pH 8.5. After the procedure to separate Th and Pa on anion exchange columns, the supernatant and washings of the $Fe(OH)_3$ precipitate were combined with the rinses of the anion exchange column and brought again to pH 10 with $NH_3$ in order to coprecipitate Be with $Mg(OH)_2$. The precipitate was dissolved in 1.5 N HCl and Mg was separated on a DOWEX $50\times8$ ion exchange column. For removal of B and Al some millilitres of saturated Na–EDTA solution were added to the 1.5 N HCl eluate of the ion exchange column, the pH was set to 4 and 20 ml acetyl–acetone were added. On the following day 20 ml of chloroform were added and the solution was stirred for 2 h whereby the Be was transferred to the chloroform phase while Al and B remained in the solution, which was separated. After addition of 20 ml 8 N HCl and by stirring for another 2 h the Be was transferred to the acid phase, separated and precipitated at pH 9 again. After several washings with distilled water to reduce the remaining amount of B in the samples the $Be(OH)_3$ was ashed to BeO at 1000°C and prepared for accelerator mass spectrometry (AMS) measurements at the AMS facility of ETH Zurich and the Paul Scherrer Institute following standard procedures. The concentrations were normalised to internal standard S555 with a nominal $^{10}$Be/$^{9}$Be ratio of $95.5\times10^{-12}$ (Table 1). The $1\sigma$ statistical uncertainties of individual samples take into account both the statistics of the $^{10}$Be 'counts' and the reproducibility of repeated measurements, which were performed for each sample. This is the reason why some of the samples, for which high water column concentrations were obtained, have larger uncertainties than others with lower concentrations.

It is noted that only the dissolved phase was analysed for $^{10}$Be concentration. For the far more particle-reactive $^{230}$Th, the particulate activity usually accounted for 5–20% of the total activity, with some values up to 38% in surface waters and up to 45% in deep waters containing resuspended material [20]. As the oceanic residence time of $^{10}$Be in the ocean is about an order of magnitude longer than that of $^{230}$Th, it is reasonable to assume that the particulate concentration of $^{10}$Be is $\leq 10\%$ of the total concentration and much less than 10% in mid-depth waters.

## 3. Results

The dissolved $^{10}$Be concentrations for all eight stations of this study increase with depth from values between non-detectable amounts and 600 atoms/g in the surface water to values between 1400 and 2000 atoms/g at depth (Fig. 2). The pattern of the $^{10}$Be distribution, in particular that of the four southern profiles, seems to resemble that of nutrient-type elements: there is a surface depletion, some increased values below the euphotic zone, constantly high values below, and sometimes a decrease again towards the bottom. A similar pattern has been observed for $^{10}$Be in other ocean basins before and has been interpreted as a consequence of adsorption/desorption processes associated with sinking and remineralisation of biogenic particulates [6]. The intermediate-depth maximum in $^{10}$Be concentration, which is most pronounced in the southernmost stations PS1772 and 227, is, however, not at the shallow

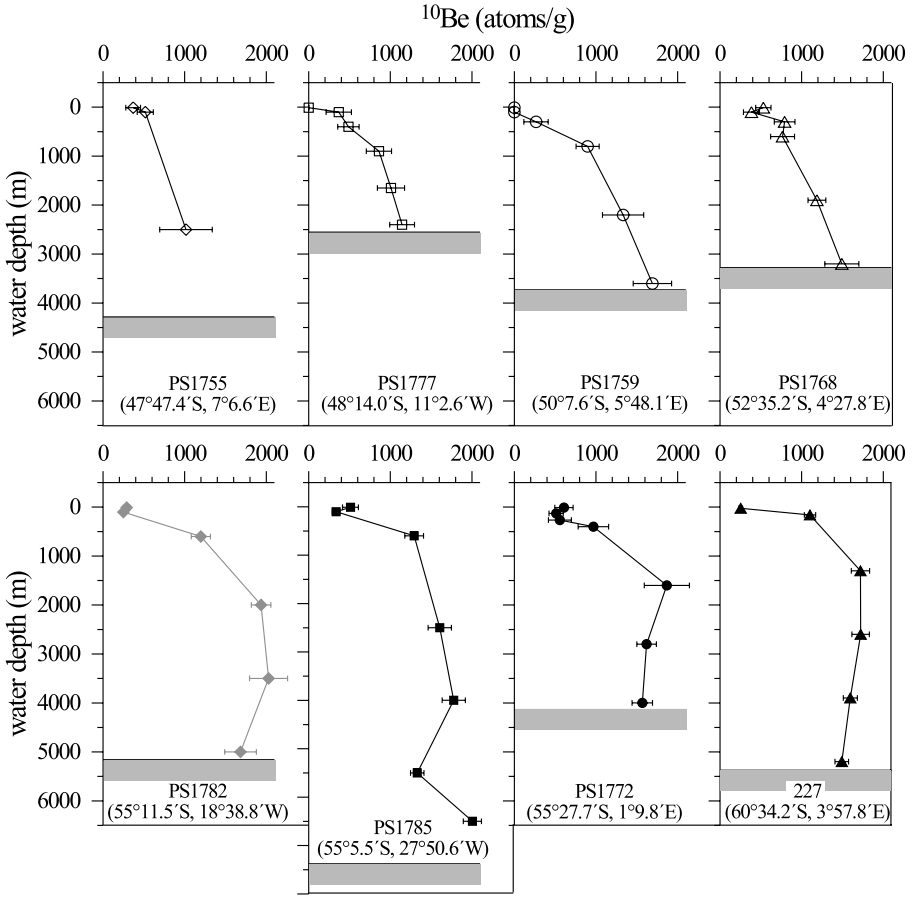


Fig. 2. Profiles of dissolved $^{10}$Be (atoms/g) against water depth (m) with 1$\sigma$ uncertainties of the AMS measurements. For each location the depth of the sea floor is given as grey bar. The data of PS1782 are given by grey line and symbols.

depths where major remineralisation of biogenic materials occurs in the Weddell Gyre [27] but rather at a depth of about 1500 m. This suggests a different origin of these $^{10}$Be variations, namely a predominant control of the different water masses with their distinct $^{10}$Be concentrations (see Section 4).

The four northern profiles from the Polar Frontal Zone and the northern Antarctic Zone show systematic differences to the southern profiles from the southern Antarctic Zone and the Weddell Sea (Fig. 2). The northern profiles show some variability in the $^{10}$Be concentrations in the uppermost 500 m but then increase linearly to the bottom. Maximum concentrations above bottom range from 1000 to 1700 atoms/g. In contrast, the southern profiles show a more rapid increase of concentration with depth, which is then either followed by constant values between 1000 m depth and the bottom or a slight decrease near the bottom. The only exception is the deepest sample from the deep profile PS1785, which shows a marked near bottom maximum. In general, the $^{10}$Be concentrations at depths greater than 1000 m are higher than in the northern profiles and range between 1400 and 2000 atoms/g.

All profiles located between 52°S and 56°S show a slight enrichment in the uppermost sample, pointing to either the precipitation-controlled atmospheric $^{10}$Be input into the ocean, which has been suggested before [3,6], or to some input from melting of icebergs in this area. No such surface

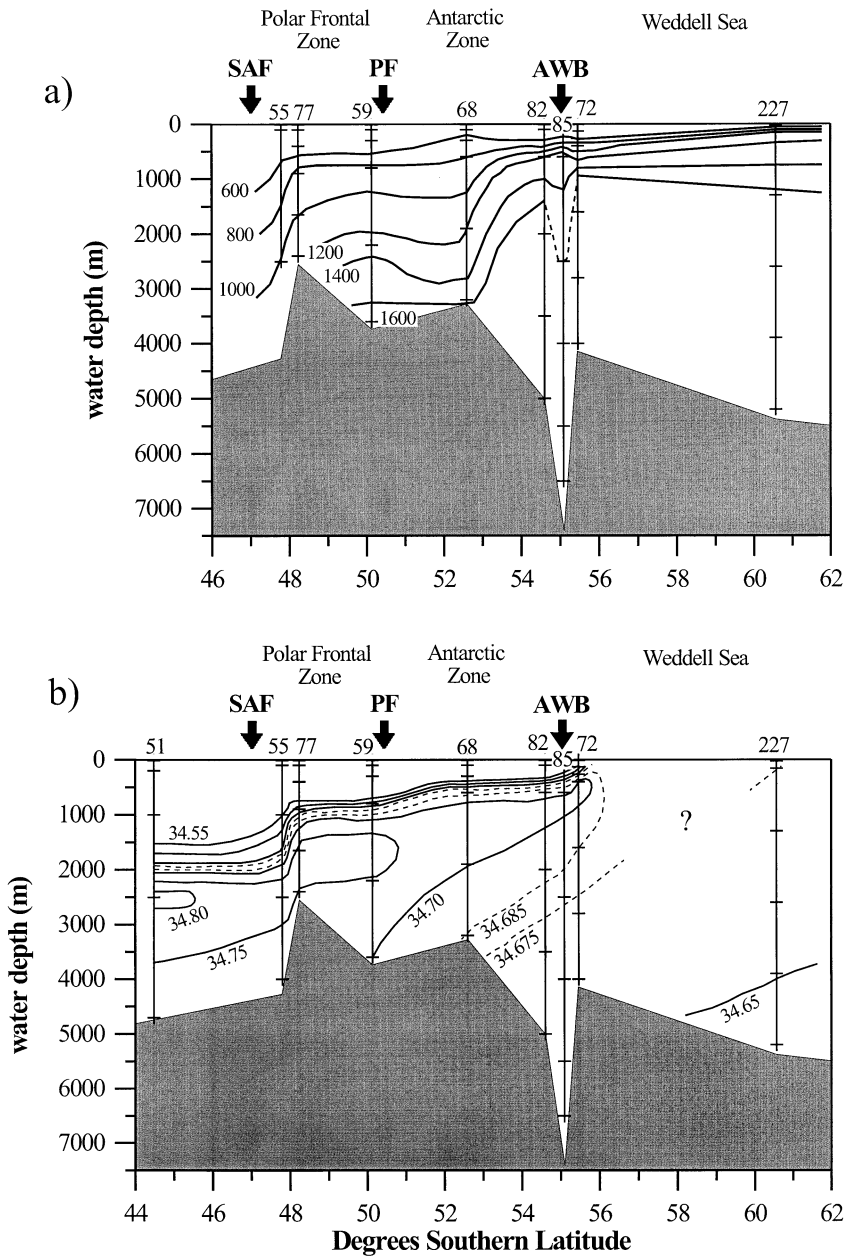


Fig. 3. (a) Dissolved $^{10}$Be concentration (atoms/g) and (b) salinity (‰) for a composite water column section between 46°S and 62°S (combining profiles from different longitudes). In panel b salinity contours between 34.55 and 34.80‰ are given in 0.05‰ steps (solid lines) and two additional contours at 34.675 and 34.685‰ are given as dashed lines. This section includes the Subantarctic Front (SAF), the Polar Front (PF) and the ACC–Weddell Gyre Boundary (AWB, position according to Whitworth and Nowlin [31]). The positions of the stations 82 and 85 which are located west of the other locations were shifted according to their positions relative to stations 68 and 72, respectively, in the $\sigma_2$ density distribution at 2000 m. Despite this adjustment the data between 1000 m and 3000 m depth at station 85 are slightly different (dashed isoline) which is due to the large distance between the stations and thus small differences in the water masses involved. Note that the morphology of the sea floor appears to be steep due to the inclusion of the two more westerly located stations, one of which is from the deep South Sandwich Trench. It is also emphasized that the southward intrusion and upwelling of the salinity maximum in panel b is entirely due to the advection of NADW.

enrichment is found in the Polar Frontal Zone and the central Weddell Sea.

## 4. Discussion

### 4.1. The distribution of $^{10}$Be in the Atlantic sector of the Southern Ocean

A previous study has shown that the dissolved $^{10}$Be concentrations in the South Atlantic are uniformly low at about 800–1000 atoms/g in NADW until the depth where Antarctic Bottom Water (AABW) is encountered, in which the concentrations increase to over 1400 atoms/g [28]. In the Pacific, $^{10}$Be concentrations are homogeneous at around 2000 atoms/g below a depth of 2000 m [6,10]. A profile of dissolved $^{10}$Be from a location in the Drake Passage close to the PF [29] shows intermediate, rather homogeneous concentrations around 1400 atoms/g throughout the water column which points to efficient vertical mixing of waters of Pacific and Atlantic origin.

The ACC in the Atlantic sector of the Southern Ocean is characterised by the southward ascent of isopycnal surfaces in three steps: at the SAF, the PF, and the AWB [30,31]. The bulk of the ACC consists of a thick layer of Circumpolar Deep Water (CDW). From the north it receives contributions from NADW at depths between 1000 and 2000, which tends to cause a division of CDW into two parts: upper (UCDW) and lower (LCDW) Circumpolar Deep Water. Deep water formation in the Weddell Sea produces Weddell Sea Deep Water (WSDW). Through mixing processes with LCDW AABW is formed, which underrides CDW at greater depth from the south. In Fig. 3 the water mass distribution is displayed as characterised by salinity measured on the same profiles as the radionuclides [20] (the water mass distribution in Fig. 3 as given by potential density would essentially look the same but would have required the introduction of different $\sigma$ values, which is why salinity was chosen here). The rising high salinity core of NADW can clearly be identified until station PS1772. The southward rising isoconcentration lines of $^{10}$Be distribution (Fig. 3) reflect the southward rising isopycnals and thus it is clear that the dissolved $^{10}$Be distribution is controlled by hydrography despite high particle fluxes between the AWB and the PF, much like the situation found previously for $^{230}$Th on the same samples [20] and also similar to recent results for $^{230}$Th, $^{231}$Pa and $^{10}$Be from the southwestern Pacific sector of the Southern Ocean [32]. This suggests that Be behaves quasi-conservatively in the Atlantic sector of the Southern Ocean. This is supported by a plot of $^{10}$Be concentration versus potential density (Fig. 4). In the density range that indicates a high proportion of NADW, $^{10}$Be concentrations are low (500–1000 atoms/g), in agreement with other $^{10}$Be data obtained for NADW [28]. At higher densities $^{10}$Be concentrations rise rapidly to values in the range of 1400–2000 atoms/g. This density range represents LCDW, a water mass consisting of high proportions of $^{10}$Be-enriched Indian and Pacific deep waters, but with some NADW admixed, which causes the $^{10}$Be concentrations to be somewhat lower than in the deep Pacific [10].

The deepest samples representing AABW/WSDW and the very dense Weddell Sea Bottom Water (WSBW) have somewhat lower $^{10}$Be concentrations than LCDW. This is probably a consequence of the admixed proportions of 'younger' water masses with lower $^{10}$Be concentrations. These 'younger' water masses, which are the main sources of dense WSBW and WSDW, either form beneath the Filchner and Ronne ice shelves [33] or originate further east, such as Warm Deep Water (WDW) [30].

### 4.2. Unusually high $^{10}$Be concentrations in the water column of the deep Weddell Sea?

When comparing the intermediate $^{10}$Be concentrations in the water column of the Drake Passage (around 1400 atoms/g) [29] with CDW in the Atlantic sector of the ACC, it appears that an additional $^{10}$Be source is required to arrive at concentrations of up to 2000 atoms/g in the southern profiles of this study. Although it is not clear how representative the Drake Passage data from a location close to the PF are as a source value for the deep ACC water masses further east (in addition, samples from different depths, such as

from 2500 to 3700 m, were combined in [29] and thus maxima in $^{10}$Be concentrations above 1500 atoms/g may have been missed), we will discuss whether additional sources or accumulation (similar to $^{230}$Th) can be invoked to explain the apparent enrichment of $^{10}$Be.

The most likely additional input source would be melting of ice originating from the Antarctic ice shelves which contains high $^{10}$Be concentrations relative to seawater (40 000–200 000 atoms/g [34]). This source was invoked by Kusakabe et al. [29] to explain the high $^{10}$Be concentrations observed in surface waters of the Drake Passage. Ice melt could influence the $^{10}$Be distribution in two different ways. The first is direct input by melting into the surface water. In the South Atlantic, icebergs drift with the clockwise circulation of the Weddell Gyre. Strong iceberg melt occurs in the region between the AWB and the PF. Near the PF the iceberg melt is thought to contribute to the local salinity minimum and may also play a role in controlling the supply of other metals such as iron to the surface waters in this area [35–37]. Our data only show very small $^{10}$Be enrichments in the surface waters of the main area of iceberg melt between 52°S and 56°S [38], which are, however, not nearly as high as the ones reported for the Drake Passage [29]. The small surface enrichments are the result of the combined effects of scavenging efficiency, precipitation, and iceberg melt. It is difficult to quantify the $^{10}$Be flux caused by the icebergs given that it is not possible to constrain the $^{10}$Be removal rates by scavenging independently. There has, however, been an estimate of Löscher et al. [36] that the contribution of melting icebergs to a salinity drop of about 0.05‰ in the vicinity of the Polar Front approximately corresponds to the admixture of 1.5‰ of water from icebergs per volume of surface water. Using $^{10}$Be concentrations in icebergs ranging from 40 000 to 200 000 atoms/g [34] this corresponds to a concentration of 60–300 atoms/g. This estimate is, however, of limited precision because the salinity decrease of 0.05 per mill is not very well defined [36]. It also has to be considered an upper limit of iceberg influence given that the salinity decrease may also partly be caused by precipitation and by melting sea ice that would supply much lower amounts of $^{10}$Be. In summary, we state that in particular in the area around the Polar Front, where a large quantity of icebergs melt and at the same time particulate scavenging is high, a contribution from iceberg melting cannot be excluded.

A second path of meltwater influence originates from melting underneath the Antarctic ice shelf. This process yields the supercooled Ice Shelf Water (ISW) which is one of the constituents of newly formed WSBW filling the deepest parts of the Weddell Sea [33]. This ice is young enough that decay of $^{10}$Be should not be significant. Our data for the four southern stations show, however, that $^{10}$Be concentrations in the deep water decline towards the seafloor, excluding WSBW as a source for enrichment of WSDW/AABW. We conclude that there is no indication for additional inputs of $^{10}$Be that contribute to the deep Weddell Gyre.

According to results by Kumar et al. [24] and Frank et al. [18] $^{10}$Be rain rates (corrected for focussing and winnowing effects using $^{230}$Th) in the uppermost sediment layer are generally close to the value expected from atmospheric production across the ACC. The only exceptions are locations from close to the AWB where values between 1.5 and $3.5\times10^9$ atoms/cm$^2$ kyr are reached (cores PS1768-8, PS1772-8 [18]; RC13-259, RC13-271 [24]). Local $^{10}$Be residence times calculated from these data (170–220 yr) are long compared with circumpolar transit time and Weddell Sea water renewal time. In Holocene sections of sediments from the Weddell Sea margin, Frank et al. [39] found a $^{10}$Be flux that is a factor of 2.5–5 above production after correction for sediment focussing ($^{10}$Be rain rates are 3.3 and $5.8\times10^9$ atoms/cm$^2$ kyr in cores PS1388-1 and PS1170-3, respectively). In a 4000 m water column with an average $^{10}$Be concentration of 1500 atoms/g this translates into a residence time on the order of 55–200 yr. The lowest residence time was obtained for core PS1388-1, which is situated in the rather productive Antarctic coastal current. For the interior Weddell Sea we expect a scavenging residence time of at least several hundred years. Thus, ventilation of the Weddell Gyre on a time scale of 35 yr [20] and transit until incor-

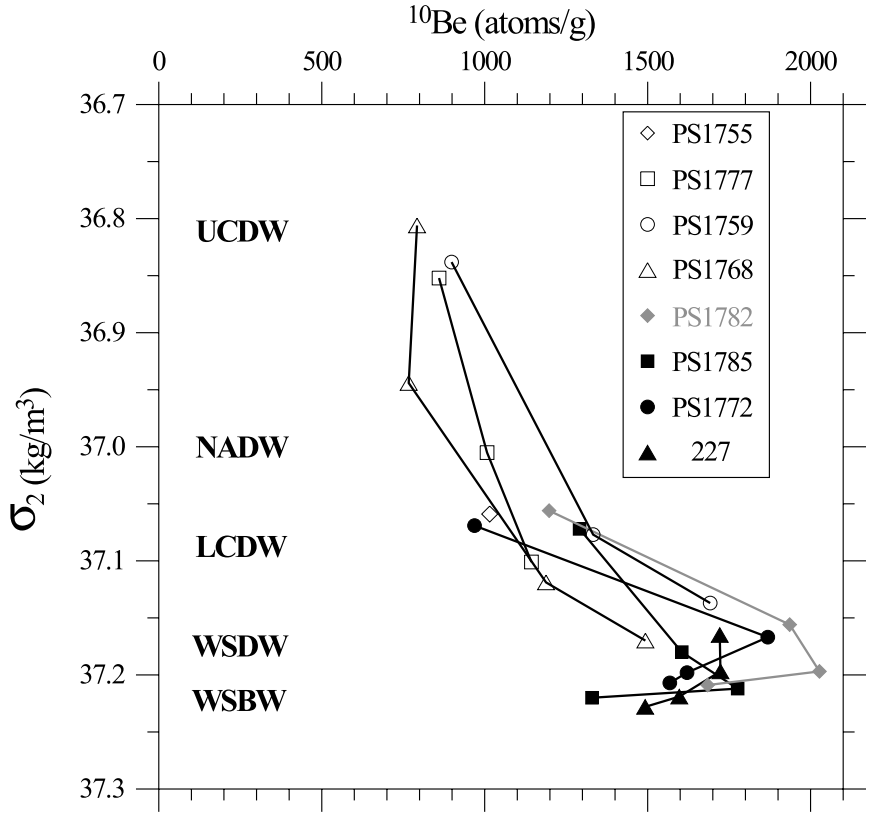


Fig. 4. $^{10}$Be concentration versus density ($\sigma_2$) for water samples deeper than 300 m. The densities of the main water masses in the Atlantic sector of the Southern Ocean are indicated for comparison.

poration into the ACC are too rapid to allow a significant effect of accumulation or scavenging on the distribution of $^{10}$Be. This is supported by the fact that in the four profiles that contain the density range of WSDW/AABW no latitudinal gradient in the $^{10}$Be concentrations is observable (Fig. 4), in contrast to the observations for $^{230}$Th [20]. Concentrations (1500–2000 atoms/g) are not lower at stations at the AWB (PS1782, PS1785) than at stations south of this front (PS1772, 227), which indicates that the transition from the low particle flux area in the south to the higher particle flux area further north is not accompanied by a decrease in $^{10}$Be concentration as is the case for $^{230}$Th [20].

These considerations suggest that the one existing depth profile of $^{10}$Be concentrations in the Drake passage [29] may not be representative and that there must be a pathway for advection of Pacific deep waters with high $^{10}$Be concentrations on the order of 2000 atoms/g into the Atlantic sector of the Southern Ocean.

### 4.3. *Use of $^{10}$Be as quasi-conservative water mass tracer in the Southern Ocean*

The data of our study clearly suggest that the $^{10}$Be concentration of particular water masses below 1000 m depth does not change significantly during transit through the Weddell Sea and during advection through the high biogenic particle flux areas of the ACC. We thus infer that $^{10}$Be can be used as a quasi-conservative reference tracer to study the behaviour of other scavenged isotopes in the Weddell Sea.

It should be noted that $^{10}$Be only behaves quasi-conservatively in intermediate and deep waters. The surface water $^{10}$Be depletion, which has not

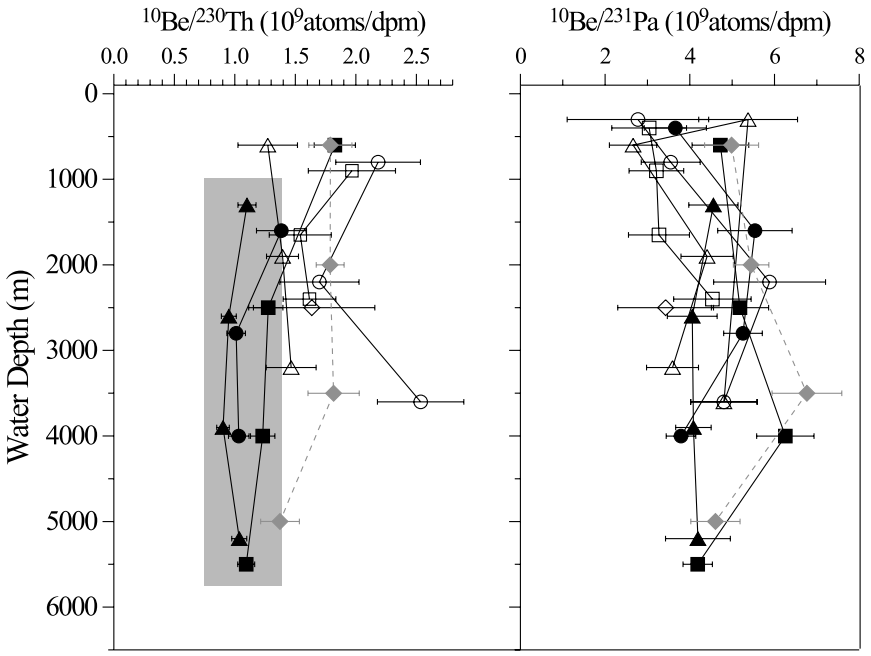


Fig. 5. Profiles of $^{10}$Be/$^{230}$Th and $^{10}$Be/$^{231}$Pa versus water depth. Symbols for the stations are the same as in the previous figures. The shaded area marks the water masses south of the AWB with a decreased $^{10}$Be/$^{230}$Th of $1.1 \pm 0.2 \times 10^9$ atoms/dpm ($1\sigma$), explained by $^{230}$Th accumulation. The data of PS 1782 are given in grey. Note that only the data below 500 m depth are displayed for the $^{10}$Be/$^{230}$Th ratios because above 500 m there is a lot of scatter, probably due to differences in scavenging processes.

been observed in such a pronounced way anywhere in the ocean before, suggests that scavenging by particles, such as biogenic opal, is important in the euphotic zone of the surface waters. This is supported by the fact that the water samples were collected during the period of the Antarctic spring bloom. One can estimate the residence time of $^{10}$Be in the uppermost 100 m of the water column by comparing the $^{10}$Be concentrations of the surface waters and the average concentrations of the complete profiles with the average residence time for the entire water depth. For the locations near the AWB, residence times in the upper 100 m between 9 and 20 months are estimated, whereas in the area of the PF the residence times appear to be rather on the order of 2–3 yr. These values are estimated assuming no additional inputs by iceberg melting, which has been suggested to be small (see Section 4.2), but would tend to reduce these estimates. These values can be compared with residence times of the most particle reactive tracer of this study, which is Th. From the PF there are $^{234}$Th data that suggest a residence time of Th in the uppermost 100 m on the order of 4 months during the period of the spring bloom [40]. Given that the ratio between the average residence times of $^{10}$Be and $^{230}$Th in deep waters of the Southern Ocean is about 10, this suggests efficient scavenging of $^{10}$Be by biogenic particles in the surface waters of the ACC. The deep water $^{10}$Be concentrations are at the same time not significantly affected, probably caused by rapid lateral advection of water masses within the ACC.

In Fig. 5 the dissolved $^{10}$Be/$^{230}$Th and $^{10}$Be/$^{231}$Pa ratios are plotted versus water depth. The three profiles from south of the AWB show significantly decreased $^{10}$Be/$^{230}$Th values in a narrow range compared with the profiles further north. This is even more apparent from Fig. 6 where $^{10}$Be/$^{230}$Th ratios for densities ($\sigma_2$) $> 36.7$ kg/m$^3$ are plotted against density for water masses deeper than 300 m. The average $^{10}$Be/$^{230}$Th for these data amounts to $1.7 \pm 0.3 \times 10^9$ atoms/dpm north

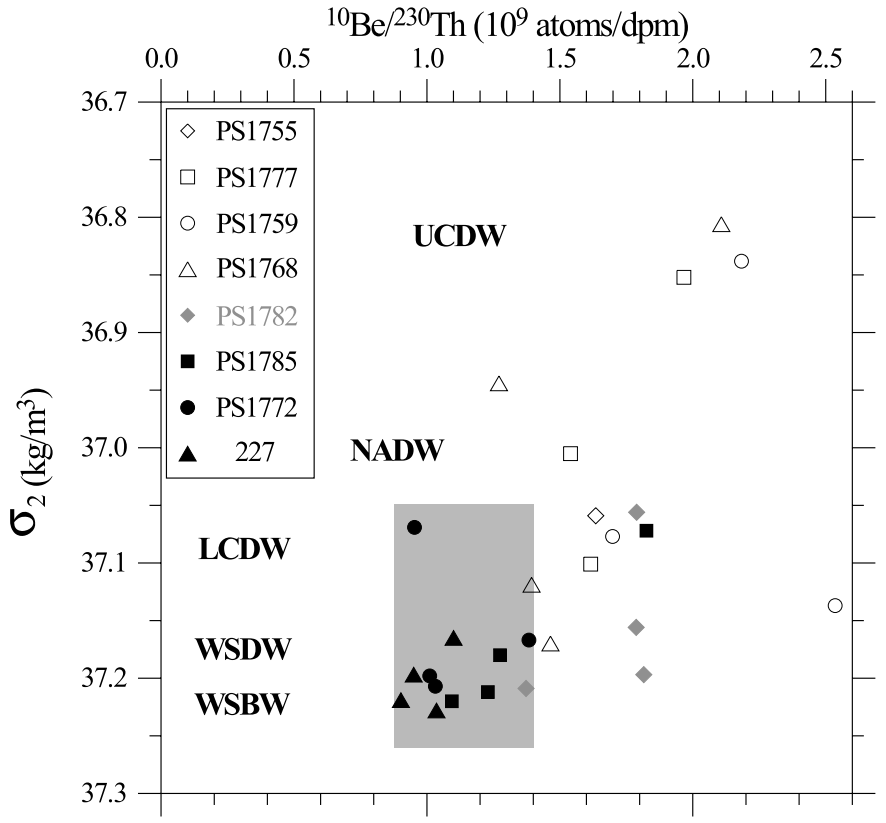


Fig. 6. $^{10}$Be/$^{230}$Th ($10^9$ atoms/dpm) versus density ($\sigma_2$) $>36.7$ kg m$^{-3}$ for water depths deeper than 300 m. The shaded area marks the water masses south of the AWB with a decreased $^{10}$Be/$^{230}$Th of $1.1\pm0.2\times10^9$ atoms/dpm ($1\sigma$), explained by $^{230}$Th accumulation. Data of PS1782 are given in grey.

of the AWB with no observable trend with depth or density. South of the AWB the ratio diminishes to $1.1\pm0.2\times10^9$ atoms/dpm, implying a significant enrichment of $^{230}$Th. This $^{230}$Th enrichment has previously been explained in terms of upwelling, ingrowth and reduced scavenging [20,21]. The normalisation to $^{10}$Be now allows it to be quantified and identified in more detail. The graph clearly shows an accumulation of $^{230}$Th in the Weddell Sea of 50% above the activity expected from conservative behaviour.

The highest total (particulate+dissolved) $^{230}$Th concentration has been observed for a AABW sample just north of the AWB (at station PS1782) [20]. The corresponding $^{10}$Be/$^{230}$Th ratio is low despite the high $^{10}$Be concentration, in accordance with the Weddell Sea origin of this water mass (potential temperature is $-0.6$°C). The samples above (3500 and 2000 m) have high $^{10}$Be concentrations and high $^{10}$Be/$^{230}$Th. These waters were obviously not enriched in $^{230}$Th in the Weddell Sea but are probably closest in composition to the deep waters entering the south Atlantic through Drake Passage (the samples of PS1782 are given in grey in the figures to visualise their somewhat exceptional composition). Station PS1785 clearly shows the influence of the $^{230}$Th enriched waters from the Weddell Sea in its low $^{10}$Be/$^{230}$Th ratios, probably because of its location south of the AWB. Station PS1768 from a comparable position relative to the AWB as PS1782, but further east is obviously less influenced by water masses enriched in $^{230}$Th, probably as a consequence of ongoing mixing of waters of Pacific origin with waters advecting from the Weddell Sea across the AWB.

When comparing the $^{231}$Pa data with $^{10}$Be and $^{230}$Th there is a lot of scatter and no clear systematic north–south difference in the $^{10}$Be/$^{231}$Pa ratio. If anything, there may be a trend of the $^{10}$Be/$^{231}$Pa values towards higher values in the southern profiles compared to the northern ones which would probably reflect the more efficient scavenging of $^{231}$Pa over $^{10}$Be. Normalisation of $^{230}$Th to $^{231}$Pa gives a similar result as normalisation to $^{10}$Be. In the mixing–scavenging model of the Weddell Sea [20] a 15% accumulation of $^{231}$Pa activity in the water column has been predicted. The scatter of the data when normalising to $^{10}$Be is too high to verify this but the results agree with the observation that $^{231}$Pa accumulation in the Weddell Sea sediments is close to its production in the water column, whereas 60% of the $^{230}$Th production is exported [21].

### 4.4. Some implications for the use of $^{10}$Be as a tracer of past particle flux and productivity

We have shown that $^{10}$Be behaves essentially conservatively in intermediate and deep waters of the Weddell Sea Atlantic sector of the ACC. This suggests that the use of $^{10}$Be as a tracer of past particle flux in the Southern Ocean is justified because the upwelling CDW will supply a constant amount of $^{10}$Be to the areas of high particle flux which is then available for scavenging in the surface waters. This is, however, only true as long as there have not been additional supplies or significant changes in the circulation patterns.

Kumar [41] suggested that the flux of $^{10}$Be to the surface waters originating from iceberg melting (see Section 4.2) may have been increased in the past as reflected by increased $^{10}$Be deposition in core RC13-259 (north of the ABW), which is located in the main area of iceberg melting [38], for periods around 185 kyr and 65–90 kyr ago (approximately 20–30 kyr after the preceding peak interglacials). He used average $^{10}$Be concentrations in Antarctic ice cores of 40 000 atoms/g [42], which is quite a conservative estimate given the range in concentrations in the Vostok Ice core [34], and an annual average of 2000 Gt of iceberg melting given by Jacobs et al. [43], to calculate an additional input of $1.6\times10^6$ atoms/cm$^2$ yr distributed over the PFZ, about equivalent to the global average atmospheric input flux ($1.2\times10^6$ atoms/cm$^2$ yr). These estimates suggest that enhanced iceberg melting, for example during surges, can increase the amount of $^{10}$Be available for scavenging significantly, possibly by up to a factor of 2. Iceberg melting was invoked to be responsible for a freshening of last glacial surface waters between 52 and 56°S [38] and may also have at least contributed to the increased $^{10}$Be deposition rates observed in Holocene sediments south of 53°S and in glacial sediments some degrees further north [24,18]. However, variations in scavenging processes and particulate fluxes have most likely been more important for the increased $^{10}$Be deposition.

During the last glacial period the overall depositional flux of $^{10}$Be into the sediments of the entire ACC north of about 52°S was enhanced by a factor of 2–3 [24,18]. This may have been accomplished in different ways: (1) the $^{10}$Be distribution in the water column was similar to present but the increased biogenic and aeolian particle fluxes caused enhanced scavenging in the northward-shifted high opaline particle flux area. This would strengthen the basis for the use of $^{10}$Be as a particle flux proxy because the concentration in the water column from which the particles scavenged $^{10}$Be has remained virtually unchanged. (2) The supply of low $^{10}$Be NADW during the last glacial was diminished or even shut down [44,45], which may have caused a predominance of $^{10}$Be-enriched water masses of Pacific origin in the ACC. The residence time of water masses in the deep Pacific with a more sluggish global thermohaline circulation was probably longer than today which would promote the development of even higher $^{10}$Be concentrations in the deep Pacific than today. The result may have been a completely different pattern of the $^{10}$Be distribution within the ACC water column with overall higher concentrations and slower exchange of water masses. Such a scenario would promote higher glacial $^{10}$Be concentrations in the water column and would thus probably also allow a higher flux of $^{10}$Be into the sediments contributing to the increase caused by enhanced particle fluxes [24,18]. Such a contribution is hard to quantify

without detailed synoptic maps of $^{10}Be/^{230}Th$ for the periods of interest but combined with increased particle fluxes that scavenged $^{10}Be$ more efficiently it may have been significant. Probably a combination of several factors (more efficient scavenging by higher biogenic and eolian particle fluxes, iceberg melting and higher $^{10}Be$ concentrations in the water column) caused the observed increased $^{10}Be$ deposition rates in the glacial Atlantic sector of the ACC although the intensity of scavenging as a function of particle flux and composition has probably been dominant. Further studies on the other factors are necessary in order to use $^{10}Be$ as tracer for past particle flux in the Southern Ocean.

## 5. Conclusions

The concentration of $^{10}Be$ in the Atlantic sector of the ACC and the Weddell Gyre resembles closely the distribution of deep water masses with elevated values in Circumpolar Deep Water and Antarctic Bottom Water and depleted values in water masses with an increased North Atlantic Deep Water component. $^{10}Be$ concentrations are obviously not modified in deep water masses, even on transit across the areas of increased particle fluxes in the opal belt. The fact that the $^{10}Be$ deposition rates below the high particle flux areas are at least equal to or higher than the fluxes expected from the atmospheric production rate suggests that there is continuous scavenging from water masses that only reside shortly above each location. The deposition of $^{10}Be$ in the ACC has thus been sensitive to changes in ocean circulation and water mass residence time in the past which complicates its use as a particle flux proxy.

The residence time of dissolved $^{10}Be$ in the Weddell Sea with respect to input and scavenging fluxes is far too long to allow a concentration change to develop in view of the 35 yr ventilation time of the Weddell Sea. $^{10}Be$ can therefore be viewed as a quasi-conservative tracer to gauge the scavenging behaviour of more particle-reactive isotopes and its use as a tracer for past particle fluxes is supported as long as supplies and ocean circulation have remained essentially the same. Normalisation of dissolved $^{230}Th$ to $^{10}Be$ confirms the $^{230}Th$ ingrowth derived previously from a model of the ventilation of the Weddell Sea. This quantitative agreement provides additional support for the conclusion that about 60% of $^{230}Th$ produced in the Weddell Sea is exported, whereas the uncertainties and the scatter in the $^{10}Be/^{231}Pa$ data do not allow improved estimates of potential $^{231}Pa$ export.

## Acknowledgements

We appreciate the constructive reviews by Catherine Jeandel, Lanny McHargue and two anonymous reviewers. We also thank Don Porcelli, Marcus Christl and Shangde Luo for discussions and acknowledge the German Science Foundation for support of the AMS $^{10}Be$ measurements. M.F. wishes to thank the Swiss National Fonds for support.*[BARD]*

## References

[1] M. Monaghan, S. Krishnaswami, K.K. Turekian, The global average production rate of $^{10}Be$, Earth Planet. Sci. Lett. 76 (1985/86) 279–287.

[2] D. Lal, B. Peters, Cosmic ray produced radioactivity on the Earth, in: Handbook of Physics 46/2, Berlin, Springer, 1967, pp. 551–612.

[3] M. Segl, A. Mangini, J. Beer, G. Bonani, M. Suter, W. Wölfli, C. Measures, $^{10}Be$ in the Atlantic Ocean, a transect at 25°N, Nucl. Instrum. Methods Phys. Res. B5 (1987) 332–334.

[4] T.L. Ku, M. Kusakabe, C.I. Measures, J.R. Southon, G. Cusimano, J.S. Vogel, D.E. Nelson, S. Nakaya, Beryllium isotope distribution in the western North Atlantic: a comparison to the Pacific, Deep-Sea Res. 37 (1990) 795–808.

[5] F. von Blanckenburg, H. Igel, Lateral mixing and advection of reactive isotope tracers in ocean basins: observations and mechanisms, Earth Planet. Sci. Lett. 169 (1999) 113–128.

[6] M. Kusakabe, T.-L. Ku, J.R. Southon, J.S. Vogel, D.E. Nelson, C.I. Measures, Y. Nozaki, Distribution of $^{10}Be$ and $^{9}Be$ in the Pacific Ocean, Earth Planet. Sci. Lett. 82 (1987) 231–240.

[7] R.F. Anderson, Y. Lao, W.S. Broecker, S.E. Trumbore, H.J. Hofmann, W. Wölfli, Boundary scavenging in the Pacific Ocean: a comparison of $^{10}Be$ and $^{231}Pa$, Earth Planet. Sci. Lett. 96 (1990) 287–304.

[8] Y. Lao, R.F. Anderson, W.S. Broecker, S.E. Trumbore,

H.J. Hofmann, W. Wölfli, Transport and burial rates of $^{10}$Be and $^{231}$Pa in the Pacific Ocean during the Holocene period, Earth Planet. Sci. Lett. 113 (1992) 173–189.

[9] F. von Blanckenburg, R.K. O'Nions, N.S. Belshaw, A. Gibb, J.R. Hein, Global distribution of beryllium isotopes in deep ocean water as derived from Fe-Mn crusts, Earth Planet. Sci. Lett. 141 (1996) 213–226.

[10] M. Kusakabe, T.-L. Ku, J.R. Southon, C.I. Measures, Beryllium isotopes in the ocean, Geochem. J. 24 (1990) 263–272.

[11] M.P. Bacon, J.N. Rosholt, Accumulation rates of $^{230}$Th and $^{231}$Pa and some transition metals on the Bermuda Rise, Geochim. Cosmochim. Acta 46 (1982) 651–666.

[12] R.F. Anderson, M.P. Bacon, P.G. Brewer, Removal of $^{230}$Th and $^{231}$Pa from the open ocean, Earth Planet. Sci. Lett. 62 (1983) 7–23.

[13] R.F. Anderson, M.P. Bacon, P.G. Brewer, Removal of $^{230}$Th and $^{231}$Pa at ocean margins, Earth Planet. Sci. Lett. 66 (1983) 73–90.

[14] S. Luo, T.-L. Ku, Oceanic $^{231}$Pa/$^{230}$Th ratio influenced by particle composition and remineralisation, Earth Planet. Sci. Lett. 167 (1999) 183–195.

[15] K. Taguchi, K. Harada, S. Tsunogai, Particulate removal of $^{230}$Th and $^{231}$Pa in the biological productive northern North Pacific, Earth Planet. Sci. Lett. 93 (1989) 223–232.

[16] H.J. Walter, M.M. Rutgers van der Loeff, H. Hoeltzen, Enhanced scavenging of $^{231}$Pa relative to $^{230}$Th in the South Atlantic south of the Polar Front: implications for the use of the $^{231}$Pa/$^{230}$Th ratio as a paleoproductivity proxy, Earth Planet. Sci. Lett. 149 (1997) 85–100.

[17] P. Sharma, P. Mahannah, W.S. Moore, T.L. Ku, J.R. Southon, Transport of $^{10}$Be and $^{9}$Be in the ocean, Earth Planet. Sci. Lett. 86 (1987) 69–76.

[18] M. Frank, R. Gersonde, M.M. Rutgers van der Loeff, G. Bohrmann, C. Nürnberg, P.W. Kubik, M. Suter, A. Mangini, Similar glacial and interglacial export bioproductivity in the Atlantic sector of the Southern Ocean: multiproxy evidence and implications for atmospheric $CO_2$, Paleoceanography 15 (2000) 642–658.

[19] Y. Lao, R.F. Anderson, W.S. Broecker, H.J. Hofmann, W. Wölfli, Particulate fluxes of $^{230}$Th, $^{231}$Pa and $^{10}$Be in the northeastern Pacific Ocean, Geochim. Cosmochim. Acta 57 (1993) 205–217.

[20] M.M. Rutgers van der Loeff, G.W. Berger, Scavenging of $^{230}$Th and $^{231}$Pa near the Antarctic Polar Front in the South Atlantic, Deep-Sea Res. I 40 (1993) 339–357.

[21] H.J. Walter, M.M. Rutgers van der Loeff, H. Hoeltzen, U. Bathmann, Reduced scavenging of $^{230}$Th in the Weddell Sea: implications for paleoceanographic reconstructions in the South Atlantic, Deep-Sea Res. I 47 (2000) 1369–1387.

[22] E.F. Yu, R. Francois, M.P. Bacon, Similar rates of modern and last-glacial ocean thermohaline circulation inferred from radiochemical data, Nature 379 (1996) 689–694.

[23] R.F. Anderson, M.Q. Fleisher, P.E. Biscaye, N. Kumar, B. Dittrich, P.W. Kubik, M. Suter, Anomalous boundary scavenging in the Middle Atlantic Bight: evidence from $^{230}$Th, $^{231}$Pa, $^{10}$Be and $^{210}$Pb, Deep-Sea Res. II 41 (1994) 537–561.

[24] N. Kumar, R.F. Anderson, R.A. Mortlock, P.N. Froelich, P.W. Kubik, B. Dittrich-Hannen, M. Suter, Increased biological productivity and export production in the glacial Southern Ocean, Nature 378 (1995) 675–680.

[25] S. Luo, T.-L. Ku, L. Wang, J.R. Southon, S.P. Lund, M. Schwartz, $^{26}$Al, $^{10}$Be and U-Th isotopes in Blake Outer Ridge sediments: implications for past changes in boundary scavenging, Earth Planet. Sci. Lett. 185 (2001) 135–147.

[26] R. Gersonde, G. Hempel, Die Expeditionen ANTARKTIS VIII/3 und VIII/4 mit FS 'Polarstern' 1989, Ber. Polarforsch. 74 (1990) 173 pp.

[27] R. Usbeck, M.M. Rutgers van der Loeff, M. Hoppema, R. Schlitzer, Shallow remineralization in the Weddell Gyre, Geochem. Geophys. Geosyst. 3 (2002) 10. 1029/2001GC000182.

[28] C.I. Measures, T.-L. Ku, S. Luo, J.R. Southon, X. Xu, M. Kusakabe, The distribution of $^{10}$Be and $^{9}$Be in the South Atlantic, Deep-Sea Res. I 43 (1996) 978–1009.

[29] M. Kusakabe, T.-L. Ku, J. Vogel, J.R. Southon, D.E. Nelson, G. Richards, Beryllium-10 profiles in sea water, Nature 299 (1982) 712–714.

[30] T. Whitworth, W.D. Nowlin, Water masses and currents of the southern Ocean at the Greenwich meridian, J. Geophys. Res. 92 (1987) 6462–6476.

[31] R.G. Peterson, T. Whitworth, The Subantarctic and Polar Fronts in relation to deep water masses through the southwestern Atlantic, J. Geophys. Res. 94 (1989) 10817–10838.

[32] Z. Chase, R.F. Anderson, M.Q. Fleisher, P.W. Kubik, Scavenging of $^{230}$Th, $^{231}$Pa, and $^{10}$Be in the Southern Ocean (SW Pacific sector): The importance of particle flux and advection, Deep-Sea Res. II (2002) submitted.

[33] A. Foldvik, T. Gammelrød, T. Tørresen, Circulation and water masses on the southern Weddell Sea shelf, in: S.S. Jacobs (Ed.), Oceanology of the Antarctic Continental Shelf, Antarctic Research Series 43, Am. Geophys. Union, Washington, DC, 1985, pp. 5–20.

[34] G.M. Raisbeck, F. Yiou, D. Bourlès, C. Lorius, J. Jouzel, N.I. Barkov, Evidence for two intervals of enhanced $^{10}$Be deposition in Antarctic ice during the last glacial period, Nature 326 (1987) 273–277.

[35] H.J.W. De Baar, J.T.M. De Jong, D.C.E. Bakker, B.M. Löscher, C. Veth, U. Bathmann, V. Smetacek, Importance of iron for plankton blooms and carbon dioxide drawdown in the Southern Ocean, Nature 373 (1995) 412–415.

[36] B.M. Löscher, J.T.M. de Jong, H.J.W. de Baar, C. Veth, F. Dehairs, The distribution of Fe in the Antarctic Circumpolar Current, Deep-Sea Res. II 44 (1997) 143–187.

[37] H.J. Dauelsberg, E. Hegner, M.M. Rutgers van der Loeff, C. Jeandel, Iron fertilization in the Southern Ocean – icebergs spawn blooms of phytoplankton, Nature (2002) submitted.

[38] L.D. Labeyrie, J.J. Pichon, M. Labracherie, P. Ippolito, J. Duprat, J.-C. Duplessy, Melting history of Antarctica during the past 60,000 years, Nature 322 (1986) 701–706.
[39] M. Frank, A. Eisenhauer, W.J. Bonn, P. Walter, H. Grobe, P.W. Kubik, B. Dittrich-Hannen, A. Mangini, Sediment redistribution versus paleoproductivity change: Weddell Sea margin sediment stratigraphy and biogenic particle flux of the last 250,000 years deduced from $^{230}Th_{ex}$, $^{10}Be$ and biogenic barium profiles, Earth Planet. Sci. Lett. 136 (1995) 559–573.
[40] M.M. Rutgers van der Loeff, K. Buesseler, U. Bathmann, I. Hense, J. Andrews, Comparison of carbon and opal export rates between summer and spring bloom periods in the region of the Antarctic Polar Front, SE Atlantic, Deep-Sea Res. I (2002) submitted.
[41] N. Kumar, Trace metals and natural radionuclides as tracers of ocean productivity, Ph.D. thesis, Columbia University, New York, 1994, 317 pp.
[42] L.R. McHargue, P.E. Damon, The global beryllium 10 cycle, Rev. Geophys. 29 (1991) 141–158.
[43] S.S. Jacobs, H.H. Hellmer, C.S.M. Doake, A. Jenkins, R.M. Frolich, Melting of ice shelves and the mass balance of Antarctica, J. Glaciol. 38 (1992) 375–387.
[44] C.D. Charles, R.G. Fairbanks, Evidence from Southern Ocean sediments for the effect of North Atlantic Deep Water flux on climate, Nature 355 (1992) 416–419.
[45] R.L. Rutberg, S.R. Hemming, S.L. Goldstein, Reduced North Atlantic Deep Water flux to the glacial Southern Ocean inferred from neodymium isotope ratios, Nature 405 (2000) 935–938.
[46] R.G. Peterson, L. Stramma, Upper-level circulation in the South Atlantic Ocean, Prog. Oceanogr. 26 (1991) 1–73.